

# Nonlinear redistribution of wealth from a Fokker-Planck description

Hugo Lima<sup>1</sup>, Allan R. Vieira<sup>1</sup>, Celia Anteneodo<sup>1,2</sup>

<sup>1</sup>*Department of Physics, PUC-Rio, Rua Marquês de São Vicente, 225, 22451-900, Rio de Janeiro, Brazil*

<sup>2</sup>*National Institute of Science and Technology for Complex Systems (INCT-SC), Rio de Janeiro, Brazil*

We investigate the effect of nonlinear redistributive drifts on the dynamics of wealth described by a Fokker-Planck equation for the probability density function  $P(w,t)$  of wealth  $w$  at time  $t$ . We consider (i) a piecewise linear tax, exempting those with wealth below a threshold  $w_0$ , and taxing the excess wealth with given rate, otherwise, and (ii) a power-law tax with exponent  $\alpha > 0$  (hence, progressive for  $\alpha > 1$  and regressive otherwise). In all cases, the collected amount of wealth is redistributed equally. We analyze how these rules modify the distribution of wealth across the population and, mainly, the inequality level measured through the Gini coefficient  $G$ . The introduction of an exemption threshold not always diminishes inequality, depending on the implementation details. Moreover, nonlinearity brings new stylized facts in comparison to the linear case, e.g., negative skewness, bimodal  $P(w,t)$  indicating stratification, or a flat shape meaning equality populated wealth layers.

## I. INTRODUCTION

The tools of statistical mechanics to tackle out-of-equilibrium processes can be useful to describe the dynamics of wealth [1]. The so-called random asset exchange models [2, 3], assuming wealth transfers through pairwise interactions between agents, have successfully shown the endogenous emergence of stylized facts of real wealth distributions such as the concentration of wealth in heavy tails and the formation of a condensed layer of the poorest people [4, 5]. In fact, rich-get-richer mechanisms can lead to the continuous accumulation of assets, accentuating wealth inequality, as observed in most countries over time [6–8]. Therefore, the effects of regulatory processes capable of counteracting or mitigating these trends are worth of investigation. With this aim, agent based [9, 10] or probabilistic approaches [11] have been considered. Alternatively, the Fokker-Planck approach is the natural counterpart of the stochastic dynamics describing asset random exchange trading. Bruce Boghosian [12, 13] derived an equation for the time evolution of the probability density of wealth  $P(w)$  that emerges from the so-called yard-sale random transfers of wealth, in which a fraction of a donor wealth is transferred to another agent [14]. In this model individuals in an artificial society possess a certain wealth and participate in transactions by pairs, such that the total net worth  $W$ , as well as the size of the population  $N$ , are conserved quantities, setting up a closed system. The impact of linear redistributive actions in such a closed economy has been addressed before [12, 13, 15–17]. Now, we consider nonlinear redistributive taxes, which can be regressive, progressive, or exempting the poorest population, and investigate how they can contribute to reduce the level of inequality.

The remaining part of the paper is organized as follows. In Sec. II, we describe the Fokker-Planck model with nonlinear drift and different settings that appear concomitantly. In Sec. III, we present numerical results for the stationary states and also for the evolution of

wealth distribution, comparing the effect of the different tax protocols, through the Gini index. Final remarks are presented in Sec. IV.

## II. FOKKER-PLANCK DESCRIPTION

The stochastic dynamics of yard-sale exchanges with taxes can be described, under certain approximations [12], through an integro-differential Fokker-Planck equation (FPE) for the probability density function (PDF) of wealth,  $P(w,t)$ , namely

$$\frac{\partial P}{\partial t} = \frac{1}{2} \frac{\partial^2}{\partial w^2} \left( [w^2 A + B] P \right) - \frac{\partial}{\partial w} (fP), \quad (1)$$

with

$$A \equiv A(w,t) = \int_w^\infty P(x,t) dx, \quad (2)$$

$$B \equiv B(w,t) = \int_0^w x^2 P(x,t) dx. \quad (3)$$

The first term in the right-hand side of Eq. (1) can be interpreted as a state-dependent diffusive spreading of wealth, which has its origin in the microscopic random exchanges between agents. In the second term, the drift  $f(w)$  represents the net gain (loss) of agents with wealth  $w$ . The derivation of this FPE with linear  $f(w)$  can be found in Ref. [12]. Now we assume that  $f(w)$  is given by

$$f(w) = \chi(\beta\bar{w} - \gamma g(w)), \quad (4)$$

where  $\gamma g(w)$  is the wealth raised from agents possessing  $w$ , through a nonlinear function  $g(w)$  times  $\gamma$ , a coefficient that can be time dependent, whereas  $\beta\bar{w}$  is the wealth received back (the same for all people), proportional to the average per capita

$$\bar{w} = \int_0^\infty xP(x,t) dx, \quad (5)$$

via a coefficient  $\beta$  that can also be time dependent, and finally  $\chi$  controls the relative strength of the drift per unit time with respect to the diffusive process.

If  $\chi = 0$ , the PDF  $P(w, t)$  continuously evolves accentuating the condensation at  $w = 0$  and the heavy Pareto power-law tail when  $w$  gets large [12], respectively meaning increase of the population at extreme poverty and concentration of wealth among a small number of people (oligarchy). This endless process that accentuates inequality can be broken by the flow of wealth from the richest to the poorest people, produced by the drift that is present when  $\chi > 0$ .

In the original version of the model,  $\beta = \gamma = 1$  and  $g(w) = w$  [12, 15], meaning time-independent taxes proportional to individual wealth. We generalize the originally linear drift in Eq. (4), by considering different kernels  $g(w)$  that are nonlinear (non proportional to  $w$ ). One of them is the piecewise-linear function

$$g(w) = (w - w_0)H(w - w_0), \quad (6)$$

where  $w_0$  is a positive constant,  $H$  is the step Heaviside function. The original version is recovered by setting  $w_0 = 0$  and  $\beta = \gamma = 1$ , in which case fees are proportional to the individual wealth no matter how small it is. We also consider the power-law taxation

$$g(w) = w^\alpha, \quad (7)$$

with  $\alpha > 0$ . The taxation can be super-linear, i.e., progressive ( $\alpha > 1$ ), or sub-linear, i.e., regressive ( $0 < \alpha < 1$ ). This protocol also includes the original case, recovered when  $\beta = \gamma = \alpha = 1$ .

Besides the specific shape of the kernel  $g(x)$ , there is another issue that must be addressed concomitantly with the drift nonlinearity. In all the analyzed cases, Eq. (1) conserves the norm of  $P(w, t)$  along time. It means conservation of the population size  $N$ , whose distribution within the full range of wealth is given by  $NP(w, t)$ . However, while in the linear case Eq. (1) naturally conserves the average wealth  $\bar{w}$  given by Eq. (5), otherwise wealth conservation must be imposed through the evolution of the drift coefficients in Eq. (4). This is important if we want to maintain the condition of a closed economy, where the total wealth  $W = N\bar{w}$  is conserved over time, without losses or accumulation, for instance, by the regulatory agency. We can let  $\gamma$  evolve in time, which means an adjustment of the protocol (setting I), or vary  $\beta$  (setting II), meaning a fixed protocol but variable retrieved wealth. Both cases and their connections are considered in the next section.

### III. PDF EVOLUTION AND STEADY STATE SOLUTION

As previously shown [12], in the absence of regulation ( $\chi = 0$ ), Eq. (1) leads to progressive condensation towards  $w = 0$ , and a heavy tail for large  $w$  develops, without actually reaching a normalizable steady state. The

inclusion of the drift with  $\chi > 0$  allows attaining a steady solution, in all the cases considered. In order to follow the time evolution of the wealth PDF, we numerically solved Eq. (1) though a standard forward-time centered-space scheme. Further details are shown in Appendix A. Alternatively, to obtain the steady state solution, we directly solved the stationary FPE, that is, setting the time derivative in Eq. (1) equal to zero, as described in Appendix B. Indeed, this solution coincides with the long-time solution of the FPE. In all numerical examples, we set  $\bar{w} = 1$ , without loss of generality, since it is equivalent to performing the change of variables  $w/\bar{w} \rightarrow w$ .

For both families of kernels  $g(w)$ , we develop in Secs. III A and III B, the setting I: fixing  $\beta = 1$  and adjusting  $\gamma$  selfconsistently. Setting II (adjustable  $\beta$  and  $\gamma = 1$ ) is discussed in Sec. III C, where we show how the steady states in both settings are related.

Finally, the wealth PDFs are characterized in terms of a widely used inequality indicator, the Gini coefficient, which can be estimated as [15],

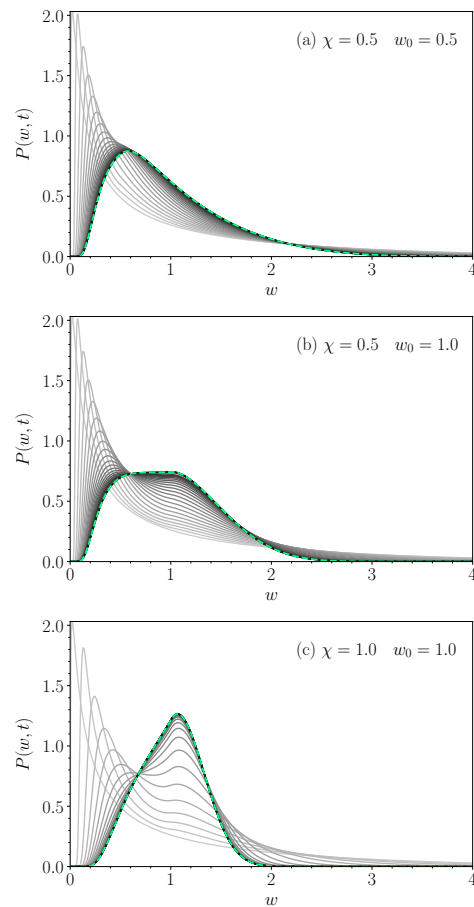


FIG. 1: **Evolution of the wealth PDF with piecewise-linear drift**, for values of  $\chi$  and  $w_0$  indicated in the legends, at times increasing (from lighter to darker) from  $t = 0$  to  $t = 2$  at each  $\Delta t = 0.1$ , and from  $t = 2$  to  $t = 5$  at each  $\Delta t = 0.5$ . The solution of the stationary FPE is also plotted (green dashed line).

$$G(t) = 1 - \frac{2}{\bar{w}} \int_0^\infty xP(x,t)A(x,t)dx. \quad (8)$$

### A. Piecewise-linear tax with exemption limit $w_0$

The evolution of  $P(w,t)$ , under the taxation ruled by the piecewise linear kernel defined in Eq. (6), is shown in Fig. 1 for different values of  $\chi$  and  $w_0$ , starting from an initial condition that results from the driftless evolution, at a time where the Gini index is  $G \simeq 0.59$ . In all cases, increasing  $\chi$  makes the final state less spread. The condensation at  $w = 0$  is suppressed, meaning the absence of a majority at extreme poverty, and the heavy tail for large  $w$  becomes restricted by a cutoff, reducing large fortunes and oligarchy. In Fig. 1a, for  $w_0 = 0.5$ , we find a picture qualitatively similar to that of the linear case [12], where the PDF has a positive skewness. Raising the threshold  $w_0$ , the PDF can become almost flat

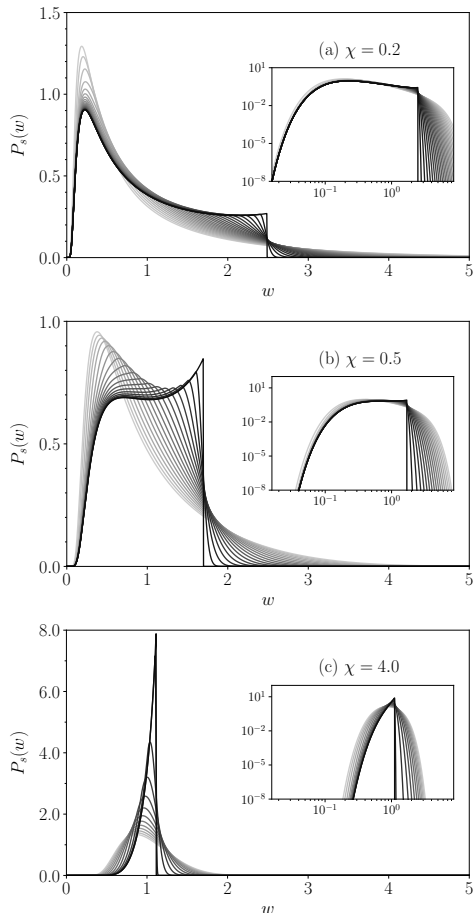


FIG. 2: **Stationary wealth PDF, with piecewise-linear drift**, for fixed  $\chi$  according to the legend, and different values of  $w_0$  varying (from light to dark lines) at each  $\Delta w_0 = 0.1$  from 0.0 up to the limiting value  $w_0 \simeq 2.5$  (a), 1.7 (b) and 1.1 (c). Inset: same data in log-log scale to exhibit the cut-offs.

(see Fig. 1b), meaning uniformly populated wealth layers. For even larger  $w_0$ , the skewness is inverted at long times, with a mode larger than the average value  $\bar{w} = 1$  (e.g., Fig. 1c). These are new features introduced by the piecewise function. The evolution of the Gini index and further details are shown in Appendix A.

The stationary PDFs for fixed  $\chi$  and a large set of values of  $w_0$  are shown in Fig. 2. Increasing the rate  $\chi$  narrows the PDF around the mean, particularly, the cut-off at low  $w$  is shifted such that wider ranges of poverty are eliminated. This behavior is also observed in the linear case and is not noticeably affected by  $w_0$  [15]. The exemption threshold  $w_0$  affects more strongly the intermediate and large- $w$  layers. The PDF can become bimodal (e.g, Fig. 2b), indicating classes with defined asset level, but scales are not well separated. The change of skewness can be observed in these plots for not too small  $\chi$  (Figs. 2b-c). Moreover, in general, raising the threshold  $w_0$  leads to a more effective cut-off such that assets that surpass that level tend to be suppressed. This is due to the flow of wealth above  $w_0$  towards the population with lower assets, depopulating the large- $w$  tail.

The long-time value  $G_s$  of the Gini index is shown for different values of  $\chi$  in Fig. 3a. It decreases by raising  $w_0$ , as expected, however, a finite minimal level is attained at a limiting value of  $w_0$ . The larger is  $\chi$ , the more sensitive is  $G_s$  to  $w_0$ . We have considered the full range of values for completeness, although some intervals of the parameters may be unrealistic. For instance, at the limiting value of  $w_0$ , the slope  $\gamma_s$  becomes divergent, to keep the average  $\bar{w}$  fixed (see Appendix A), and the PDF

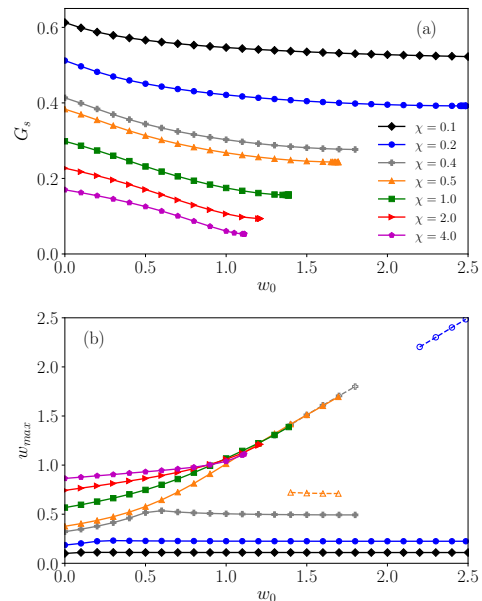


FIG. 3: (a) **Stationary Gini index** for different values of  $\chi$  as a function of  $w_0$ . (b) **Mode of the wealth PDF** (filled symbols) vs.  $w_0$ . The second maximum, when it exists, is also plotted (hollow symbols). Lines are a guide to the eye.

becomes truncated as can be observed in Fig. 2.

In Fig. 3b, we plot the mode,  $w_{max}$  (filled symbols), as well as the second maximum (hollow symbols) whenever it exists. For low values of  $\chi$ , the mode is weakly sensitive to  $w_0$  and remains below  $\bar{w}$  (e.g., case  $\chi = 0.2$ ), producing positively skewed distributions. For larger  $\chi$ , the mode is shifted towards the line  $w_{max} = w_0$ , and can exceed the mean value  $\bar{w}$  (unity, in our examples). When a second peak at larger  $w$  develops (which occurs for not too large  $\chi$ ), it can become the mode as  $w_0$  increases (e.g., for  $\chi = 0.5$  in Fig. 3b, and also see Fig. 2b).

## B. Power-law taxation

Stationary PDFs for different values of  $\alpha$  and  $\chi$  are exhibited in Fig. 4. As in the piecewise-linear case, there is a narrowing of the PDF with increasing  $\chi$ . Flat, bimodal, and negatively skewed PDFs can also emerge when  $\alpha > 1$ , but the PDF shapes are smoother for the power-law kernel and the cutoffs less sharp.

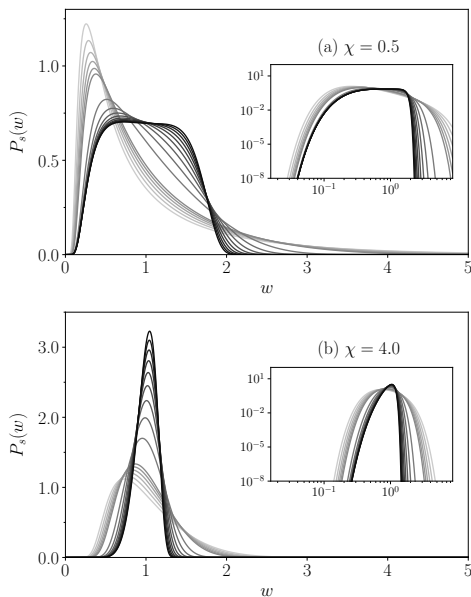


FIG. 4: **Stationary wealth PDF, for power-law drift**,  $P_s(w)$ , for different values of  $\alpha$  at each  $\Delta\alpha = 0.1$  for  $\alpha \in [0.5, 0.9]$ , and  $\Delta\alpha = 1$  for  $\alpha \in [1, 10]$ , with values of  $\chi$  according to the legend. Inset: same data in log-log scale to show the cutoff.

The stationary values of index  $G$  vs.  $\alpha$ , for fixed values of  $\chi$ , are presented in Fig. 5a. When comparing these curves with the respective ones of the piecewise-linear case in Fig. 3a, we notice a matching for  $\alpha \simeq 4w_0 \gtrsim 1$ . While the progressive taxation with  $\alpha > 1$  emulates better the tax with exemption threshold  $w_0$ , we find the main differences for  $\alpha < 1$ , due to its regressive character. In the limit  $\alpha \rightarrow 0$ , due to the requirement of wealth

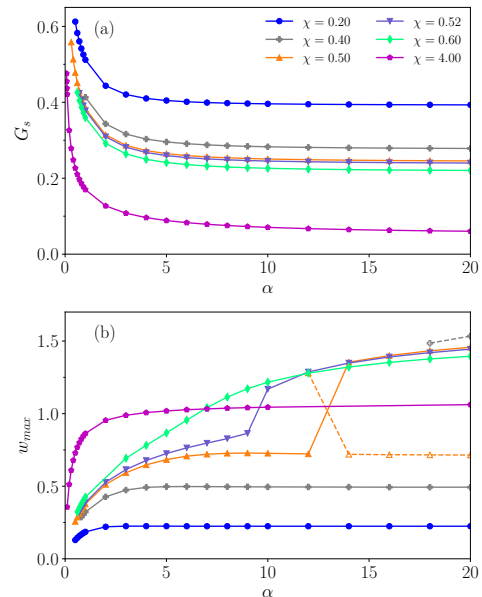


FIG. 5: (a) **Stationary Gini index** for different values of  $\chi$  as a function of  $\alpha$ . (b) **Mode of the stationary wealth PDF** (filled symbols) vs.  $\alpha$ . The second maximum, when it exists, is also plotted (hollow symbols). Full lines are a guide to the eye.

conservation, from Eq. (1), we have

$$\int_0^\infty wP(w, t)dw = \gamma \int_0^\infty P(w, t)dw, \quad (9)$$

yielding constant  $\gamma = \bar{w}$ . Then

$$f(w) = \chi(\bar{w} - \gamma) = 0 \Rightarrow \frac{\partial}{\partial w}[fP] = 0, \quad (10)$$

implying that the FPE drift term goes to zero when  $\alpha \rightarrow 0$ . Therefore, the dynamics evolves towards condensation and long tails. Even though, the sublinear kernel does produce relatively low values of the Gini index for large enough  $\chi$ . In fact,  $G_s$  rapidly decreases with  $\alpha$  in the regressive case. With regard to the maxima shown in Fig. 5, the mode overcomes the average  $\bar{w}$  and a second maximum can appear only for very large values of the exponent  $\alpha$ .

## C. Setting II

Up to now, we developed the setting I, fixing the amount of wealth shared (by fixing  $\beta = 1$ ) and adapting the coefficient  $\gamma(t)$  to conserve the average wealth. Now, we analyze setting II, where  $\gamma = 1$  and  $\beta$  is adjusted. The stationary solutions can be related by identifying each drift terms in Eq. (4), yielding

$$\begin{aligned} \beta_s^{II} &= 1/\gamma_s^I \\ \chi^{II} &= \chi^I \gamma_s^I. \end{aligned} \quad (11)$$

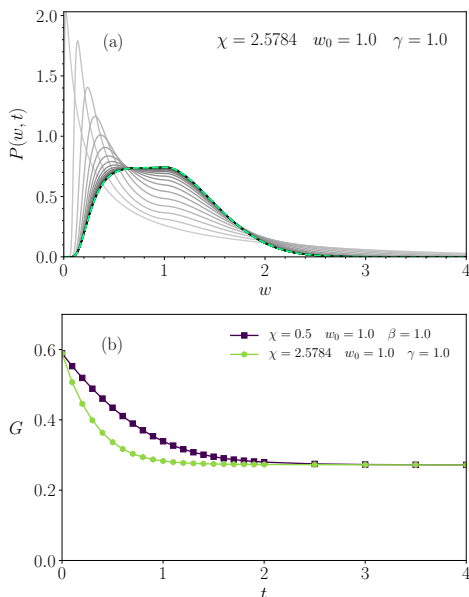


FIG. 6: **Setting II: evolution for piece-wise linear drift.** (a) Wealth PDF (a),  $P(w, t)$  vs.  $w$ , with variable  $\beta$ , for the same times used in Fig. 1. (b) Gini index vs. time for settings I (black) and II (light green), with parameters verifying Eqs. (11) leading to the same steady state).

As an illustration, we followed the evolution of case

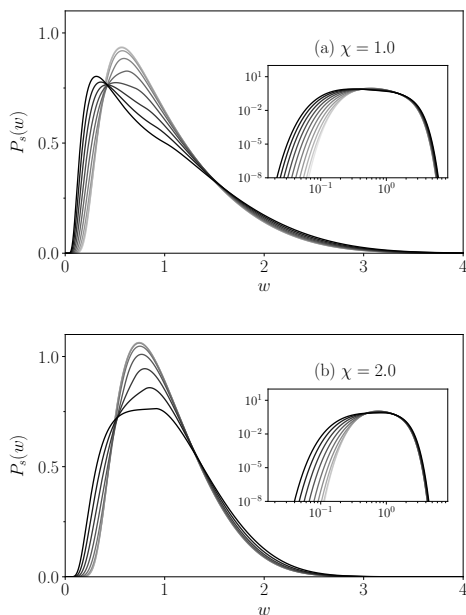


FIG. 7: **Setting II: stationary wealth PDF with piecewise-linear drift**, for fixed  $\chi$  according to the legend, and different values of  $w_0$  varying (from light to dark lines) at each  $\Delta w_0 = 0.1$  from 0.0 up to 1.0 in (a) and from 0.0 up to 0.9 in (b). Inset: same data in log-log scale to exhibit the cut-offs.

II, with parameters that verify the above relations with respect to setting I in Fig. 1b. In fact, the steady state coincide (compare Figs. 1b and 6a). However, the temporal evolution differs, as can be also observed by following the Gini indexes over time, in Fig. 6b. The steady state is reached faster within setting II.

In contrast to setting I, where increasing the threshold  $w_0$  reduces the inequality measured by  $G_s$ , in setting II, a different dependence on  $w_0$  emerges, as shown in Fig. 6b. The stationary value of the Gini index is rather insensitive to  $w_0$  and even increases with  $w_0$ . A high threshold exempts people with lower level of wealth but the collected wealth is smaller. Then it is better to remove the exemption. The corresponding steady PDFs are presented in Fig. 7. For the power-law taxation, the Gini index decreases with  $\alpha$  (not shown).

Of course, in the limit  $w_0 \rightarrow 0$  or  $\alpha \rightarrow 1$ , yielding the linear case, both setting coincide.

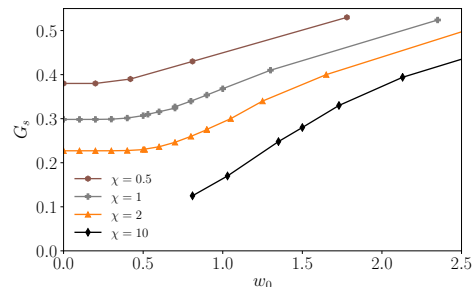


FIG. 8: **Stationary Gini index for setting II** as a function of  $w_0$ . Lines are a guide to the eye.

#### IV. FINAL REMARKS

Regulatory processes seem to be necessary to counteract concentration trends. We studied nonlinear redistributive mechanisms that allow to reduce inequality. Two families of taxation kernels were studied: piecewise linear, with an exempting threshold, and power law. We performed numerical integration of the FPE to follow the time evolution of  $P(w, t)$ , starting from a given initial unequal distribution and also the stationary PDF  $P_s(w)$  was directly obtained.

These studied tax protocols produce economic mobility against the natural trend towards the condensation at  $w = 0$  that occurs in the regulation-free case. The nonlinearity brings new features with respect to the linear case, allowing to achieve greater social equality. Moreover, distributions with peculiar stylized facts can emerge. For moderate values of the control parameters, distributions can be bimodal, which indicates the stratification and coexistence of the population in economic classes with distinct characteristic asset levels. A flat profile can also emerge, and, for strong regulation, the skewness of the

wealth PDF changes sign. We also discussed the similarities and differences between two settings, where either the collected or the divided wealth coefficients are adjusted. Depending on the adjustment made, a higher exemption threshold  $w_0$  can be detrimental for equality.

Let us also remark that the results can be translated to those of arbitrary  $\bar{w}$  by a simple scaling. In fact, from Eq. (1), we have  $P(w, t; \bar{w}) = P(w/\bar{w}, t; 1)/\bar{w}$ , together with the identifications:  $w_0(1) = w_0(\bar{w})/\bar{w}$  (and  $\gamma$  unchanged) in the piecewise-linear case, and  $\gamma(1) = \gamma(\bar{w})\bar{w}^{\alpha-1}$  in the power-law case.

As a perspective for future work, it would be inter-

esting to study the underlying agent exchange dynamics, the effect of redistribution applied at discrete time steps, the combination of a power-law kernel with exemption threshold  $w_0$ , and also the impact of the spatial dimension [18] going beyond the mean-field approximation.

We acknowledge partial financial support by the Coordenação de Aperfeiçoamento de Pessoal de Nível Superior - Brazil (CAPES) - Finance Code 001. C.A. also acknowledges partial support by Conselho Nacional de Desenvolvimento Científico e Tecnológico (CNPq). We thank Bruce Boghosian for elucidating methods used in his previous works.

- 
- [1] A. Dragulescu, V.M. Yakovenko, Statistical mechanics of money, *Eur. Phys. J. B* 17, 723 (2000).
- [2] M. Patriarca, E. Heinsalu, A. Chakraborti, Basic kinetic wealth-exchange models: common features and open problems, *Eur. Phys. J. B* 73, 145 (2010).
- [3] *Econophysics of Wealth Distributions: Econophysics-Kolkata I* ed. by A. Chatterjee, S. Yarlagadda, B.K. Chakraborti. Springer Science & Business Media (2005).
- [4] C.F. Moukarzel, S. Goncalves, J.R. Iglesias, M. Rodriguez-Achach, and R. Huerta-Quintanilla, Wealth condensation in a multiplicative random asset exchange model, *EPJ Special Topics* 143, 75 (2007).
- [5] J. Li, B. Boghosian, C. Li, The Affine Wealth Model: An agent-based model of asset exchange that allows for negative-wealth agents and its empirical validation, *Physica A* 516, 423 (2019).
- [6] [https://en.wikipedia.org/wiki/List\\_of\\_countries\\_by\\_wealth\\_equality](https://en.wikipedia.org/wiki/List_of_countries_by_wealth_equality)
- [7] B.M. Boghosian, Is Inequality Inevitable?, *Scientific American*, Nov. 1 (2019).
- [8] T. Piketty, *Le Capital Au XXe Sicle* (ditions du Seuil, 2013).
- [9] Z. Burda, P. Wojcieszak, K. Zuchniak, Dynamics of wealth inequality, *C. R. Physique* 20, 349363 (2019)
- [10] B.-H. F. Cardoso, S. Goncalves, and J. R. Iglesias, Wealth distribution models with regulations: dynamics and equilibria, *Physica A* 124201 (2020).
- [11] C. Chorro, A simple probabilistic approach of the Yard-Sale model, *Statistics and Probability Letters* 112, 35 (2016).
- [12] B. Boghosian, Kinetics of wealth and the Pareto law, *Phys. Rev. E* 89, 042804 (2014).
- [13] B. Boghosian, FokkerPlanck description of wealth dynamics and the origin of Pareto's law, *IJMP C* 25, 1441008 (2014).
- [14] B. Hayes, Follow the money, *Am. Sci.* 90, 400 (2002).
- [15] B. Boghosian, A. Devitt-Lee, M. Johnson, J. Li, J.A. Marq, H. Wang, Oligarchy as a phase transition: The effect of wealth-attained advantage in a FokkerPlanck description of asset exchange, *Physica A* 476, 15 (2017).
- [16] J. Lie, B. Boghosian, Duality in an asset exchange model for wealth distribution describes a very interesting duality symmetry of this Fokker-Planck equation, *Physica A* 497, 154 (2018).
- [17] B. M. Boghosian, A. Devitt-Lee, H. Wang, Describing realistic wealth distributions with the extended Yard-Sale

model of asset exchange, arXiv:1604.02370v1 (2016).

- [18] J. Novotný, On the measurement of regional inequality: does spatial dimension of income inequality matter?, *Ann. Reg. Sci.* 41, 563580 (2007).

## Appendix A: Numerical integration of the FPE

In order to obtain the solution of Eq. (1) numerically, we performed the change of variables

$$w = -\ln(1 - y), \quad (\text{A1})$$

that univocally maps the interval  $[0, +\infty)$  into the interval  $[0, 1]$  [15]. With this change, Eqs. (2)-(5) become

$$A(y, t) = \int_y^\infty \frac{P(w(x), t)}{1 - x} dx, \quad (\text{A2})$$

$$B(y, t) = \int_0^y \frac{\ln^2(1 - x)}{1 - x} P(w(x), t) dx, \quad (\text{A3})$$

$$f(y, t) = \chi\left(\beta\bar{w} - \gamma g(w(y))\right), \quad (\text{A4})$$

$$\bar{w} = -\int_0^1 \frac{\ln(1 - y)}{(1 - y)} P(w(y), t) dy. \quad (\text{A5})$$

Additionally, the normalization condition, meaning conservation of the population size, becomes

$$\int_0^1 \frac{P(w(y), t)}{1 - y} dy = 1. \quad (\text{A6})$$

Then, Eq. (1) can be rewritten as

$$\frac{\partial P}{\partial t} + (1 - y) \frac{\partial C}{\partial y} = (1 - y) \left\{ (1 - y) \frac{\partial^2 D}{\partial y^2} - \frac{\partial D}{\partial y} \right\}, \quad (\text{A7})$$

where  $C$  and  $D$  are

$$C \equiv C(y, t) = f(y, t)P, \quad (\text{A8})$$

$$D \equiv D(y, t) = \frac{1}{2} (\ln^2(1 - y) A + B) P. \quad (\text{A9})$$

Equation (A7) was integrated using a standard forward-time centered-space algorithm.

In setting I,  $\beta = 1$  and  $\gamma$  evolves satisfying

$$\gamma(t) \int_0^\infty g(w)P(w,t)dw = \bar{w}, \quad (\text{A10})$$

which means conservation of the total wealth owned by the individuals (or average wealth per individual, since the population size is conserved).

In setting II,  $\gamma = 1$  and  $\beta$  is ruled by

$$\beta(t)\bar{w} = \int_0^\infty g(w)P(w,t)dw. \quad (\text{A11})$$

For the piecewise-linear case, the time evolution of  $\gamma$  within setting I is shown in Fig. 3a, and that of the Gini index in Fig. 3b. In the absence of regulation ( $\chi = 0$ ), condensation would proceed, leading to dramatic inequality, with the Gini index monotonically increasing. Differently, for  $\chi > 0$ , the Gini index stabilizes. Depending on the initial condition, this stabilization can occur from below (e.g., for  $\chi = 0.05$ ), or moving far from the condensed state towards a more fair distribution of wealth for large enough  $\chi$ . While the initial rate of decrease depends on  $\chi$ , the final stabilization value is ruled by  $w_0$  too. Of course, for an initial PDF with sharp cutoff below  $w_0$ , the drift will be ineffective.

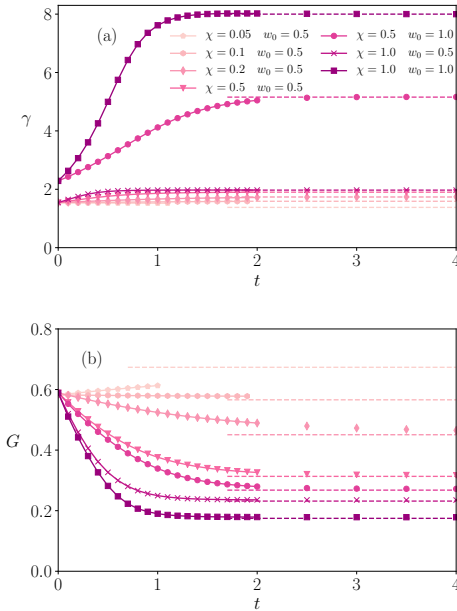


FIG. 9: (a) Time evolution of  $\gamma$ , from the numerical integration of FPE (1), for the values of  $\chi$  and  $w_0$  of Fig. 9. The long-time value of  $\gamma$  is in good agreement with that obtained by direct integration of the stationary FPE. (b) Evolution of the Gini index  $G(t)$ . Dotted lines indicate the steady state values. The computational cost increases when reaching the drift-less limit  $\chi = 0$ .

## Appendix B: Direct integration of the steady FPE

In the particular case of the linear rule  $g(w) = w$ , recovered for  $w_0 = 0$  or  $\alpha = 1$ , we have  $\beta = \gamma = 1$ , independently of the value that  $\chi > 0$  assumes, and also independently of time, hence the stationary value is  $\gamma_s = 1$  (or  $\beta_s = 1$ ).

Otherwise, the stationary value  $\gamma_s$  was obtained self-consistently from the integration of the stationary form of the FPE (1), which for no flux boundary conditions reads

$$\frac{1}{2}\mu' - fP = 0, \quad (\text{B1})$$

where  $\mu \equiv \mu(w) = (w^2A + B)P(w)$  and “ $r$ ” mean differentiation with respect to  $w$ .

In order to solve this equation, we generalized the numerical procedure described in Ref. [15]. It consists in splitting Eq. (B1) into the following coupled linear differential equations, namely,

$$A' = -P = -\mu/(w^2A + B), \quad (\text{B2})$$

$$B' = w^2P = w^2\mu/(w^2A + B), \quad (\text{B3})$$

$$\mu' = 2fP = 2f\mu/(w^2A + B), \quad (\text{B4})$$

with the initial conditions  $A(0) = 1$ ,  $B(0) = \mu(0) = 0$ , together with the normalization condition, namely,  $A_0 = \lim_{w \rightarrow \infty} A(w) = 0$ . This integration however is not straightforward due to the singular behavior of  $P(w)$

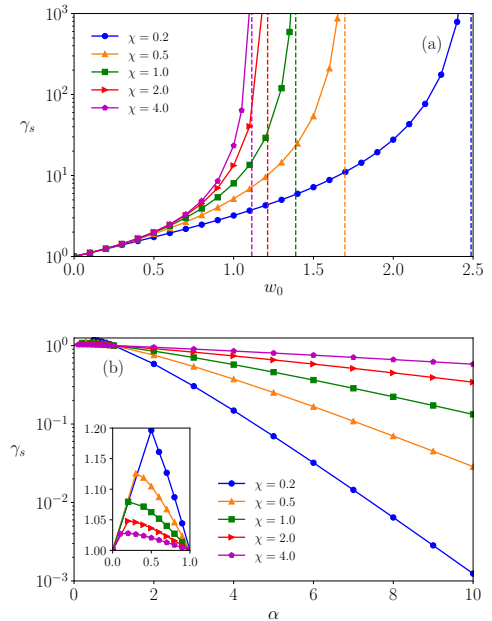


FIG. 10: Stationary value of  $\gamma$  as a function of  $w_0$  (a) and  $\alpha$  (b), for different values of  $\chi$  indicated in the legend. In (a), the vertical dotted lines indicate the asymptote. In (b), the inset is a zoom of the vicinity of the origin. Full lines are a guide to the eye.

near the origin, that behaves as

$$P(w) \simeq \frac{C}{w^2} \exp\left(2 \int^w \frac{f(x)}{x^2} dx\right), \quad (\text{B5})$$

where  $C$  is a constant. Then, we use the final value in the interval  $(0, \delta w)$ , with  $\delta w \ll 1$  as initial condition for the set of differential equations (B2)-(B4). But still, this initial condition depends on  $C$ , which must be determined from the normalization constraint  $A_0 = \lim_{w \rightarrow \infty} A(w) = 0$ . From the plot of  $A_0(C)$  vs.  $C$ , using a Newton-Raphson (NR) procedure,  $C$  can be determined by solving  $A(C) = 0$ , which has a single root. This is, essentially, the procedure described before for the linear case [15]. In the nonlinear case, we must still determine the value of  $\gamma_s$  (in setting I) or  $\beta_s$  (in setting II) that defines  $f(w)$ , under the constraint of conservation of the average wealth  $\bar{w}$ . Then, a second NR procedure is required to find the correct value of  $\gamma_s$  or  $\beta_s$  for each value of  $C$  that enters in the first NR scheme. (Actually in numerical integration, we also use the change of variables given by Eq. (A1).) The steady solutions  $P_s(w)$  found through this procedure are in accurate agreement

with the long-time solutions obtained by numerical integration of the time-dependent FPE, as illustrated in the insets of Figs. 1 and 7.

For fixed  $\beta = 1$  (setting I), the stationary value of  $\gamma_s$  is plotted in Fig. 10, for given values of  $\chi$ , as a function of  $w_0$  (a) and  $\alpha$  (b). In case (a),  $\gamma_s$  increases from unity at  $w_0 = 0$  (pure linear case) diverging at a finite value  $w_{0c}$  (indicated by dotted vertical lines), following the scaling  $\gamma_s \sim (w_{0c} - w_0)^{-2}$ . This divergence implies a truncation of the PDF at the critical value  $w_{0c}$ , as observed in Fig. 4. For the power-law rule, the coefficient  $\gamma$  plays a different role. The curves first increase from  $\gamma_s = 1$ , up to a maximal value, and then decay exponentially towards zero. Notice that when,  $\alpha = 1$  (pure linear case),  $\gamma_s = 1$ . When  $\alpha = 0$ , from Eq. (10), we have  $\gamma = \bar{w}$  ( $= 1$  in our examples). As a consequence the drift term with redistributive mechanism vanishes, then we recover the dynamics without tax regulation when the system becomes at long time an oligarchy of wealthy people concomitantly with a condensed phase of the very poor ones (see inset of Fig. 10). The computational cost increases when reaching the drift-less limit.